

Review of Recent Tevatron Jet, W/Z +Jet and Heavy-flavor Production Results

Shin-Shan Yu

On behalf of the CDF and DØ Collaborations

Fermi National Accelerator Laboratory, P.O. Box 500, Batavia, IL 60510, USA

DOI: will be assigned

This paper reviews several recent measurements at the Fermilab Tevatron, including cross sections for inclusive jet, dijet production, cross sections for electroweak boson (W or Z) production in association with inclusive or heavy-flavor (b or c) jets, and b -jet shapes. In addition, searches for new physics using the dijet angular distributions are discussed. These analyses are based on integrated luminosities of 0.3–2.5 fb⁻¹ of $p\bar{p}$ collisions at $\sqrt{s} = 1.96$ TeV, collected with the CDF and DØ detectors. The results directly test the leading order and next-to leading order calculations of perturbative quantum chromodynamics and provide constraints on the parton distribution functions and physics beyond the standard model.

1 Introduction

Measurements using jet final states have been of great interest to both experimentalists and theorists for the following reasons. First, among high p_T physics processes at a hadron collider, jet production has the largest cross section. Therefore, jet production can test perturbative quantum chromodynamics (pQCD) with the highest reach in energy and rapidity (y). Second, measurements at the Tevatron, which are complementary to the measurements by HERA and fixed target experiments, may constrain parton distribution functions (PDFs) in the region of large Q^2 and medium-to-large x and reduce uncertainties on the gluon, b , and s quark PDFs. Measurements will have greater impacts on PDFs when the uncertainties on the cross sections due to variation of renormalization and factorization scales (pQCD uncertainties) are much smaller compared to the uncertainties from existing PDFs, *e.g.* measurements of inclusive jet cross section. Third, these measurements not only provide stringent tests of the standard model (SM) physics, but also probe physics beyond the SM. The production of W or Z in conjunction with inclusive or heavy-flavor jets is one of the major backgrounds to searches for SM Higgs, SUSY, and other models. Measurements of the cross sections of these processes decrease uncertainties on the estimation of backgrounds. The angular distributions of jet events, which are not very sensitive to PDFs, can also probe the presence of new physics.

Section 2 briefly describes the jet definition and reconstruction algorithms used at the Tevatron. Sections 3–10 discuss the results of these analyses. Section 11 gives the conclusion.

2 Jet Definition and Reconstruction

Jets are collimated sprays of particles originating from quarks or gluons. The most common jet reconstruction algorithms at the Tevatron are midpoint cone and k_T .¹ The midpoint cone and k_T algorithms cluster objects² based on their proximity in the geometry and momentum space, respectively. The midpoint cone algorithm starts from objects above an energy threshold (seeds) and sums the four-momentum vectors of all objects within a cone of radius R_{cone} ³ around the seed. The total four-momentum vector of these objects defines a new jet axis. The process is iterated until the updated jet axis is within a tolerance from the previous jet axis; a stable cone is formed. Then, additional seeds are added at the midpoints between all pairs of stable cones whose separation is less than $2R_{\text{cone}}$ and the clustering procedure is repeated using these additional seeds. Finally, geometrically overlapping cones are split or merged depending on the amount of shared momentum. The k_T algorithm starts by considering every object as a protojet and calculates $k_{T,i}^2$ for each protojet and $k_{T(i,j)}^2$ for each pair of protojets.⁴ All $k_{T,i}^2$ and $k_{T(i,j)}^2$ are then collected into a single sorting list. If the smallest in this list is $k_{T,i}^2$, protojet i is promoted to a jet and removed from the list. If the smallest is $k_{T(i,j)}^2$, protojets i and j are combined into a single protojet. The procedure is iterated until the list is empty. The cone algorithm has simpler underlying event and multiple interaction corrections while the k_T algorithm is less sensitive to higher order perturbative QCD effects. More discussions of the strengths and weaknesses of these two algorithms are in Ref. [1].

Three levels of energies are defined, (i) parton level: the true energy of the parent parton (quark or gluon), (ii) particle level: the total true energy of all particles contained in a jet, including underlying event and products of fragmentation and hadronization, but excluding the energy from multiple $p\bar{p}$ interactions per crossing, (iii) detector level: energy measured in the calorimeters. The cross sections discussed here are presented as functions of particle-level energy.⁵ Calorimeters may under- or over-measure the energies of particles due to finite resolution, non-uniformity, and inefficiency of detector. Programs that provide theoretical predictions of cross sections at the next-to leading order (NLO) typically do not include parton showering. Therefore, in order to have a valid comparison between data and theory, corrections have to be applied. For measurements in data, corrections of energy from the detector to the particle level follow the procedures described in Ref. [2, 3].⁶ For theory predictions, corrections of energy from the parton to the particle level are obtained by comparing PYTHIA or HERWIG MC with parton shower and fragmentation switched on vs. switched off.⁷

¹When comparing data and theory, the same algorithms are applied.

²In data, the “object” is a calorimeter cell with energy deposit. In theory, the “object” is a parton.

³ $R_{\text{cone}}^2 \equiv \Delta y^2 + \Delta\phi^2$.

⁴Here, $k_{T,i}^2 \equiv p_{T,i}^2$ and $k_{T(i,j)}^2 \equiv \min(p_{T,i}^2, p_{T,j}^2)\Delta R_{i,j}^2/D^2$, where $R_{i,j}$ is the distance between the two protojets in the $y - \phi$ space and D is a parameter that controls the size of the jet.

⁵The energy at the particle level depends only on physics models, not detectors.

⁶The corrections are $\approx 20\%$ (50%) of the jet energy at 50 GeV and $\approx 10\%$ (20%) at 400 GeV for CDF(DØ).

⁷The corrections are $\approx 10\text{--}20\%$ at 50 GeV and drops quickly to below 5 % when energy is above 100 GeV.

3 Measurements of Inclusive Jet Cross Section

As mentioned in Section 1, inclusive jet production cross section provides constraints on the gluon PDF.⁸ The inclusive jet cross section from Tevatron Run I [4] had excess in data with respect to NLO predictions at high p_T . Data had been included later in the global fits of CTEQ6 and MRST2001 and preferred larger contribution of gluons at high x . At Run II, CDF and DØ have measured inclusive jet cross section with midpoint cone [5, 6] and k_T algorithms [7]. The Run II measurements have extended the cross section reach significantly both in p_T and rapidity (y). The midpoint seeds are added⁹ in the cone algorithm in order to reduce sensitivity to non-perturbative effects, such as radiation of soft gluons.

The cross section is measured as a function of corrected jet p_T (to the particle level), in 5–6 bins of jet rapidity. Dominant sources of systematic uncertainties are jet energy scale¹⁰ and jet energy resolution. Measurements in data are compared to NLO predictions and CTEQ6.1M PDFs for CDF, CTEQ6.5M PDFs for DØ. The renormalization and factorization scales (μ_R and μ_F) are set to $0.5p_T^{\text{jet}}$ for CDF and p_T^{jet} for DØ. Figure 1 and Figure 2 show the ratios of Run II data to theory using the cone algorithm and k_T algorithm, respectively. Although the PDFs and scales used are not exactly the same, all three measurements have a similar trend: at high p_T and large $|y|$ (equivalent to large x), the data prefer smaller values of cross section than the theory prediction. The CDF k_T and DØ cone measurements are already included in the global fit of MSTW2008 PDFs; not only the uncertainties of gluon component have decreased, but also the central values. There is an ongoing effort to include the CDF cone measurement and update CTEQ PDFs as well.

4 Measurements of Dijet Mass Spectra and Search for New Particles Decaying into Dijets

Measurements of dijet mass spectra provide an alternate method to constrain PDFs. In addition, new particles predicted by physics beyond SM may appear as resonances in the dijet mass spectra. These new particles and decays include: (i) $q^* \rightarrow qg$ (quark compositeness [8]), (ii) axigluon or coloron $\rightarrow q\bar{q}$ (chiral color model [9]), (iii) color-octet techni- ρ (ρ_{T8}) $\rightarrow q\bar{q}$ or gg (extended and topcolor-assisted technicolor [10]), (iv) Randall Sundrum graviton $\rightarrow q\bar{q}$ or gg (warped extra dimension [11]), (v) W' (Z') $\rightarrow q\bar{q}'(q\bar{q})$ (grand unified theories GUT [12]), (vi) diquark $\rightarrow qq$ or $\bar{q}\bar{q}$ (E_6 GUT [13]). The CDF measurement of dijet mass spectrum [14] requires both jets to be central ($|y^{\text{jet}}| < 1.0$) while the DØ measurement [15] is performed in six bins of $|y|$ and extended to $|y|_{\text{max}} = 2.4$, where $|y|_{\text{max}}$ is the rapidity of the jet with the largest $|y|$ among the two leading jets (see Figure 3).¹¹ Both CDF and DØ have not seen significant discrepancy from the NLO predictions and the results are yet to be included in the global PDF fits. While the limits on W' , Z' , and RS graviton are not as stringent as those obtained by the lepton channels, CDF has set the world's best limits and excluded at 95% C.L. the mass of q^* at 260–870 GeV/ c^2 , of axigluon and coloron at 260–1250 GeV/ c^2 , of ρ_{T8} at 260–1100 GeV/ c^2 , and of E_6 diquark at 260–630 GeV/ c^2 . The DØ limits are work in progress.

⁸The inclusive jet cross section measured in the forward region will be most sensitive to gluon PDF since new physics is expected to appear mostly in the central region.

⁹There were no midpoint seeds at Run I.

¹⁰The uncertainty on the jet energy scale is 2–3(1.2–2)% for CDF(DØ).

¹¹Ordered in jet p_T .

5 Search for New Physics in the Dijet Angular Distributions

An excess in data may indicate presence of new physics, but may also imply that the PDFs have to be updated; matrix elements for hard scattering processes and PDFs are entangled in the calculation of absolute production cross sections. Instead, the shapes of angular distributions, which are disentangled from PDFs, are more sensitive to new physics. The shape of the dijet angular variable, χ_{dijet} ¹², is flat for Rutherford scattering, and is more strongly peaked at small value of χ_{dijet} in the presence of new physics;¹³ the peak fraction increases as the dijet mass M_{jj} increases. CDF has focused on $M_{jj} = 0.55\text{--}0.95 \text{ TeV}/c^2$ and looked at the ratio of the number of events in two χ_{dijet} regions: $N_{1 < \chi_{\text{dijet}} < 10} / N_{15 < \chi_{\text{dijet}} < 25}$, for four M_{jj} bins [16]. DØ has a wider mass range¹⁴, 0.25–above 1.10 TeV/c^2 , and has studied the normalized χ_{dijet} distributions for ten M_{jj} bins (see Figure 3) [17]. Since no significant discrepancy is observed between the data and SM prediction, both experiments set limits on the compositeness scales [8], Λ_C , which characterizes the physical size of composite states. DØ has obtained the world’s best limits: $\Lambda_C > 2.84$ (2.82) TeV for the interference term $\eta = +1$ (-1), assuming flat prior in the new physics cross section. DØ also set limits on ADD large extra dimension [18] and TeV^{-1} extra dimension [19].

6 Measurement of W + Inclusive Jet Cross Section

CDF has used early Run II data and measured the W + jet cross section [20]. While most jet cross section measurements have major uncertainties from the jet energy scale, this measurement also suffers from the uncertainty on the background estimate at large jet p_T and high jet multiplicity; this is the region where top pair production dominates. Measured results are compared with NLO predictions from MCFM and two different schemes of interfacing leading-order (LO) matrix element with parton shower generators and jet matching (MLM:ALPGEN+HERWIG+MLM, SMPR: MADGRAPH+PYTHIA+CKKW). Both LO and NLO predict well the cross section ratios of different jet multiplicity σ_n/σ_{n-1} . The NLO predictions also have good agreement with the measurement, both in shape and absolute cross section, as functions of jet multiplicity and jet E_T . As expected, the LO tends to under-predict the absolute cross section. Among the two LO schemes, SMPR has better agreement at low E_T due to a better underlying event model in PYTHIA.

7 Measurements of W + Heavy-flavor Jet Cross Section

The production of W boson in association with heavy-flavor jets is one of the major backgrounds to searches for new physics (*e.g.* Higgs). A sample of W boson with heavy-flavor jets may be obtained by requiring the jets to contain either secondary vertices (SECVTX tagging) or a soft electron or muon (soft lepton tagging).

¹²Here, $\chi_{\text{dijet}} \equiv (1 + \cos \theta^*) / (1 - \cos \theta^*)$, where $\cos \theta^* = \tanh(y^*)$, $\pm y^*$ is the rapidity of each jet in the center-of-mass frame, and $y^* = \frac{1}{2}(y_1 - y_2)$.

¹³Here, the new physics models refer to quark compositeness, large extra dimension, and TeV^{-1} extra dimension.

¹⁴This is the same dataset that is used to measure the dijet mass spectrum, as described in Section 4.

CDF has measured the $W + b$ jet production cross section, where the measurement is proportional to the number of b jets and restricted to the kinematic range: a charged lepton with $p_T > 20$ GeV/ c and $|\eta| < 1.1$, a neutrino with $p_T > 25$ GeV/ c , and one or two jets regardless of species with $E_T > 20$ GeV and $|\eta| < 2.0$ [21]. This definition of cross section has been chosen in order to minimize uncertainties on the acceptance. The jets are tagged by ultra-tight SECVTX [22].¹⁵ The fraction of tagged jets originating from b quarks is extracted by fitting the mass reconstructed at the secondary vertices to templates of light, c , and b -flavor jets (see Figure 4). The cross section has been measured to be $2.74 \pm 0.27(stat) \pm 0.42(syst)$ pb, which is ≈ 3.5 times larger than the LO prediction of 0.78 pb from ALPGEN. The NLO calculations are available, but not yet implemented in an MC program that allows comparison of data and theory with user-defined kinematic requirements.

CDF and DØ have also studied samples of W boson with single charm candidate by tagging the charm quark with soft muon tagging [23, 24]. While SECVTX and soft lepton taggings could help separating heavy-flavor from light-flavor jets, a separation between b and c requires more advanced analysis techniques, such as neural network. Nevertheless, one could employ the fact that in $W +$ single charm events, the muon from semileptonic decays of c hadrons and the charged lepton from W decays are oppositely charged, therefore, with a large asymmetry in the number of oppositely-charged vs. same-charged events, while background from $Wb\bar{b}$ or $Wc\bar{c}$ has zero asymmetry. CDF has measured the absolute cross section for $W \rightarrow \ell\bar{\nu}_\ell$, $p_T^e > 20$ GeV/ c , and $|\eta^c| < 1.5$ to be 9.8 ± 3.2 pb. DØ has measured the cross-section ratio, $\sigma(W+c)/\sigma(W+jet)$ for jet $p_T > 20$ GeV/ c and $|\eta| < 2.5$, to be $0.074 \pm 0.019(stat)_{-0.014}^{+0.012}(syst)$, and also measured the ratios as a function of jet p_T . Both experiments have found good agreement between data and LO or NLO predictions within uncertainties. Since the dominant process of Wc production is $gs \rightarrow Wc$, future Wc cross section measurements with reduced uncertainties may constrain the s quark PDF.

8 Measurements of $Z +$ Inclusive Jet Cross Section

The measurements of Z boson production in association with inclusive jets contain only small amount of background from mis-identified leptons and are one of the cleanest channels to test pQCD. CDF has measured the $Z +$ jet cross section as functions of jet multiplicity and jet E_T [25]. In addition, DØ has measured the cross section as a function of Z boson kinematics: $p_T(Z)$ and $y(Z)$, and the angular separation between Z and jets: $\Delta\phi(Z, jet)$, $\Delta y(Z, jet)$, and $y_{boost}(Z + jet)$ [26, 27, 28]. Both CDF and DØ have seen good agreements between data and theory when NLO predictions are available. DØ has also compared their results with a number of LO matrix element generators and pure parton showering programs, such as ALPGEN, SHERPA, PYTHIA, HERWIG. Overall, the LO MC programs under-predict the cross sections, but the programs that interface matrix element generator with parton shower MC have better agreement with data in shapes. The results of these comparisons may provide inputs to the MC generation for LHC experiments.

¹⁵The ultra-tight SECVTX is operated at a different point from the standard SECVTX [22] and further decreases the light (charm) backgrounds by a factor of 10 (4), at the expense 50% reduction in b -tagging efficiency.

9 Measurement of $Z + \text{Heavy-flavor Jet}$ Cross Section

CDF has measured the ratio of $Z+b$ jet cross section to inclusive Z cross section [29]. Measuring the ratio, instead of the absolute cross section, makes the systematic uncertainties from luminosity and lepton identification largely cancel. Analysis requires at least one jet tagged by the standard SECVTX algorithm and the b fraction is extracted by fitting the secondary vertex mass as described in Section 7. The per jet cross section ratio, $\sigma^{\text{jet}}(Z + b \text{ jet})/\sigma(Z)$, for $E_T^{b \text{ jet}} > 20$ GeV, $|\eta^{b \text{ jet}}| < 1.5$, $76 < M_{\ell\ell} < 106$ GeV/ c^2 , has been measured to be $(3.32 \pm 0.53(\text{stat}) \pm 0.42(\text{syst})) \times 10^{-3}$. Although the measured results are consistent with predictions from MCFM, the predictions have a large dependence on scales, which is unexpected for NLO calculations. For example, the cross section ratio at $N_{\text{jet}} = 2$ for $Q^2 = \langle p_{T,\text{jet}}^2 \rangle$ is a factor of two of the prediction for $Q^2 = m_Z^2$. Several investigations show that MCFM does not provide full NLO predictions for one of the production diagrams: $q\bar{q} \rightarrow Zb\bar{b}$ when only one b jet is observed.¹⁶ Similar to the case of $W + b$ cross section, NLO calculations are available, but not yet implemented in an MC program that allows user-defined kinematic requirements. The other dominant production process is gluon initiated, $gb \rightarrow Zb$ ¹⁷, therefore, future $Z + b$ cross section measurements may constrain the b quark PDF.

10 Measurement of b -jet Shapes

The jet shape $\Phi(r)$ is defined as the fraction of momentum carried by particles within a cone of radius r , relative to the total momentum within the jet cone size R . By definition, $\Phi(R)$ is equal to one. The b -jet shapes provide an alternate method to probe the $b\bar{b}$ production mechanism, particularly the fraction of gluon splitting, which is complementary to the measurement of the $b\bar{b}$ angular correlation. A b -jet that originates from only one b quark has narrower¹⁸ jet shape than a b -jet that originates from two b quarks; gluon splitting tends to produce more 2- b -quark jets. The CDF measurement has been compared to predictions by PYTHIA and ALPGEN, with the default 1- b -quark fraction f_{1b} , only one b quark, only two b quarks, and with $f_{1b} - 0.2$ [30]. Data have shown a preference over $f_{1b} - 0.2$ (see Figure 4).

11 Conclusion

Measurements of inclusive jet, dijet mass, $W/Z + \text{inclusive jet}$ cross sections provide stringent tests of pQCD and are in agreement with NLO predictions. The Run II inclusive jet cross section results have decreased the central value and uncertainty of gluon PDF at high x . The dijet mass spectrum and angular distributions have been used to set the world's best limits on parameters predicted by new physics, such as mass of excited quark, axigluon/coloron, and compositeness scale, *etc.* Measurement of b -jet shape suggests that the fraction of gluon-splitting for $b\bar{b}$ production has to be increased in PYTHIA and HERWIG. More data are being collected at the Tevatron and 8 fb^{-1} of $p\bar{p}$ collisions are expected by the end of 2010. Updates with more data will benefit the $W/Z + \text{heavy flavor}$ measurements and also push the other analyses to a wider kinematic range. In addition, full NLO predictions for $W/Z + \text{heavy flavor}$

¹⁶When the two b quarks are collinear, they may be reconstructed as single b jet. When the two b quarks are well separated, one of them may be outside of the detector acceptance.

¹⁷Equivalent to $gg \rightarrow Zb\bar{b}$.

¹⁸Narrower jet shape means more momentum at small r .

in a user-friendly MC program will give more sensible data and theory comparisons. As the QCD productions of these processes are well measured and studied, our chance of discovery will be enhanced due to the better understanding of backgrounds.

12 Acknowledgments

I would like to thank the CDF and $D\bar{0}$ QCD conveners and the authors of each individual analysis, for answering my endless questions.

References

- [1] S. D. Ellis, J. Huston, K. Hatakeyama, P. Loch, and M. Tonnesmann, *Prog. Part. Nucl. Phys.* **60**, 484 (2008).
- [2] A. Bhatti *et al.*, *Nucl. Instrum. Meth. A* **566**, 375 (2006).
- [3] M. A. Voutilainen, Ph.D. thesis, University of Helsinki, 2008.
- [4] F. Abe *et al.* (CDF Collaboration), *Phys. Rev. Lett.* **77**, 438 (1996); B. Abbott *et al.* (D0 Collaboration), *Phys. Rev. Lett.* **82**, 2451 (1999).
- [5] A. Abulencia *et al.* (CDF Collaboration), *Phys. Rev. D* **74**, 071103 (2006); T. Aaltonen *et al.* (CDF Collaboration), *Phys. Rev. D* **78**, 052006 (2008) and Erratum-ibid. *D* **79**, 119902 (2009).
- [6] V. M. Abazov *et al.* (D0 Collaboration), *Phys. Rev. Lett.* **101**, 062001 (2008).
- [7] A. Abulencia *et al.* (CDF Collaboration), *Phys. Rev. Lett.* **96**, 122001 (2006); A. Abulencia *et al.* (CDF Collaboration), *Phys. Rev. D* **75**, 092006 (2007) and Erratum-ibid. *D* **75**, 119901 (2007).
- [8] U. Baur, I. Hinchliffe, and D. Zeppenfeld, *Int. J. Mod. Phys. A* **2**, 1285 (1987); U. Baur, M. Spira, and P. M. Zerwas, *Phys. Rev. D* **42**, 815 (1990).
- [9] P. H. Frampton and S. L. Glashow, *Phys. Lett. B* **190**, 157 (1987); J. Bagger, C. Schmidt, and S. King, *Phys. Rev. D* **37**, 1188 (1988); R. S. Chivukula, A. G. Cohen, and E. H. Simmons, *Phys. Lett. B* **380**, 92 (1996); E. H. Simmons, *Phys. Rev. D* **55**, 1678 (1997).
- [10] K. D. Lane and M. V. Ramana, *Phys. Rev. D* **44**, 2678 (1991); K. Lane and S. Mrenna, *Phys. Rev. D* **67**, 115011 (2003).
- [11] L. Randall and R. Sundrum, *Phys. Rev. Lett.* **83**, 3370 (1999).
- [12] E. Eichten, I. Hinchliffe, K. D. Lane, and C. Quigg, *Rev. Mod. Phys.* **56**, 579 (1984) and Addendum-ibid. **58**, 1065 (1986).
- [13] J. L. Hewett and T. G. Rizzo, *Phys. Rept.* **183**, 193 (1989).
- [14] T. Aaltonen *et al.* (CDF Collaboration), *Phys. Rev. D* **79**, 112002 (2009).
- [15] <http://www-d0.fnal.gov/Run2Physics/WWW/results/prelim/QCD/Q14/>
- [16] http://www-cdf.fnal.gov/physics/new/qcd/dijetchi_08/
- [17] V. M. Abazov *et al.* (D0 Collaboration), arXiv:0906.4819.
- [18] N. Arkani-Hamed, S. Dimopoulos, and G. R. Dvali, *Phys. Lett. B* **429**, 263 (1998); D. Atwood, S. Bar-Shalom, and A. Soni, *Phys. Rev. D* **62**, 056008 (2000).
- [19] K. R. Dienes, E. Dudas, and T. Gherghetta, *Nucl. Phys. B* **537**, 47 (1999); A. Pomarol and M. Quiros, *Phys. Lett. B* **438**, 255 (1998); K. m. Cheung and G. L. Landsberg, *Phys. Rev. D* **65**, 076003 (2002).
- [20] T. Aaltonen *et al.* (CDF Collaboration), *Phys. Rev. D* **77**, 011108 (2008).
- [21] http://www-cdf.fnal.gov/physics/new/qcd/wbjets_1900_public/index.html
- [22] D. E. Acosta, *et al.* (CDF Collaboration), *Phys. Rev. D* **71**, 052003 (2005); C. Neu, FERMILAB-CONF-06-162-E.
- [23] T. Aaltonen *et al.* (CDF Collaboration), *Phys. Rev. Lett.* **100**, 091803 (2008).

- [24] V. M. Abazov *et al.* (D0 Collaboration), Phys. Lett. B **666**, 23 (2008).
- [25] T. Aaltonen *et al.* (CDF Collaboration), Phys. Rev. Lett. **100**, 102001 (2008);
http://www-cdf.fnal.gov/physics/new/qcd/zjets_08/public.html.
- [26] V. M. Abazov *et al.* (D0 Collaboration), Phys. Lett. B **669**, 278 (2008).
- [27] V. M. Abazov *et al.* (D0 Collaboration), Phys. Lett. B **678**, 45 (2009).
- [28] <http://www-d0.fnal.gov/Run2Physics/WWW/results/prelim/QCD/Q12/>
- [29] T. Aaltonen *et al.* (CDF Collaboration), Phys. Rev. D **79**, 052008 (2009).
- [30] T. Aaltonen *et al.* (CDF Collaboration), Phys. Rev. D **78**, 072005 (2008).

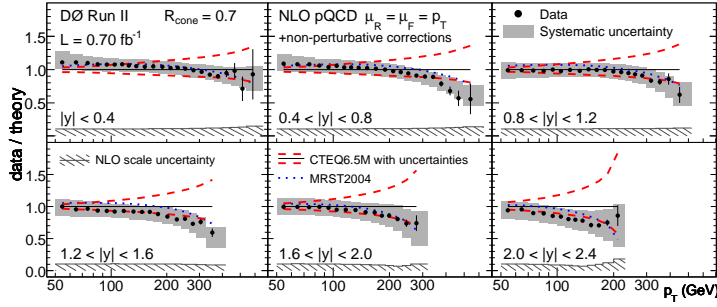
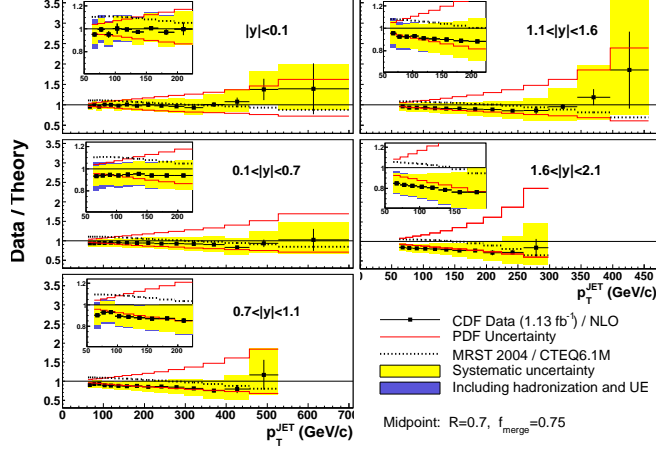


Figure 1: The Tevatron Run II results of inclusive jet cross section using midpoint cone algorithm. Ratios of CDF (top) and DØ (bottom) data to NLO theory are shown.

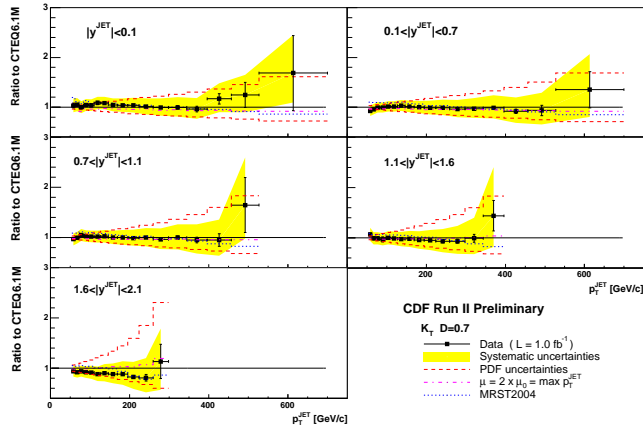


Figure 2: The Tevatron Run II results of inclusive jet cross section using k_T algorithm. Ratios of CDF data to NLO theory are shown.

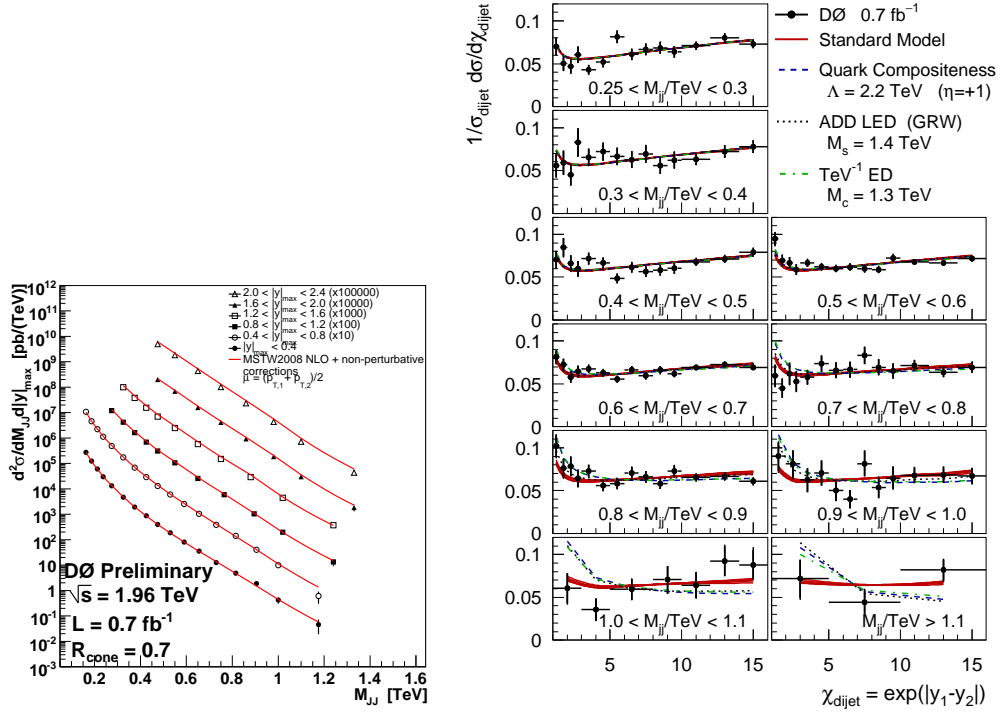


Figure 3: Measurements of dijet mass spectra by DØ (left) and normalized χ_{dijet} distributions from the DØ data, SM, and new physics predictions (right).

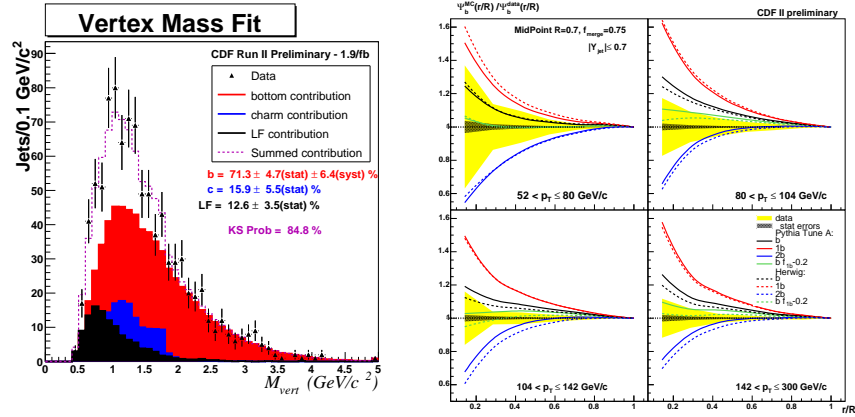


Figure 4: Fitting of secondary vertex mass measured in CDF data to templates of light, c , and b -flavor jets (left). The CDF measurement of b -jet shape in four p_T bins, and predictions from PYTHIA and HERWIG with various 1- b -quark fractions (right).